We are IntechOpen, the world's leading publisher of Open Access books Built by scientists, for scientists

4,800
Open access books available

122,000
International authors and editors

135M
Downloads

Our authors are among the

154
Countries delivered to

TOP 1%
most cited scientists

12.2%
Contributors from top 500 universities

CLARIVATE ANALYTICS BOOK CITATION INDEX INDEXED

WEB OF SCIENCE™

Selection of our books indexed in the Book Citation Index in Web of Science™ Core Collection (BKCI)

Interested in publishing with us?
Contact book.department@intechopen.com

Numbers displayed above are based on latest data collected.
For more information visit www.intechopen.com

6

Possibilities of Usage LBIC Method for Characterisation of Solar Cells

Jiri Vanek and Kristyna Jandova
Brno University of Technology
Czech Republic

1. Introduction

Light Beam Induced method works on principle of exposure very small area of a solar cell, usually by laser beam focused directly on the solar cell surface. This point light source moves over measured solar cell in direction of both X and Y axis. Thanks to local current - voltage response the XY current - voltage distribution in investigated solar cell can be measured. Acquainted data are then arranged in form of a current map and the behaviour of whole solar cell single parts is thus visible. Most common quantity measured by Light Beam Induced method is Current (LBIC) which is set near local I_{SC} current.

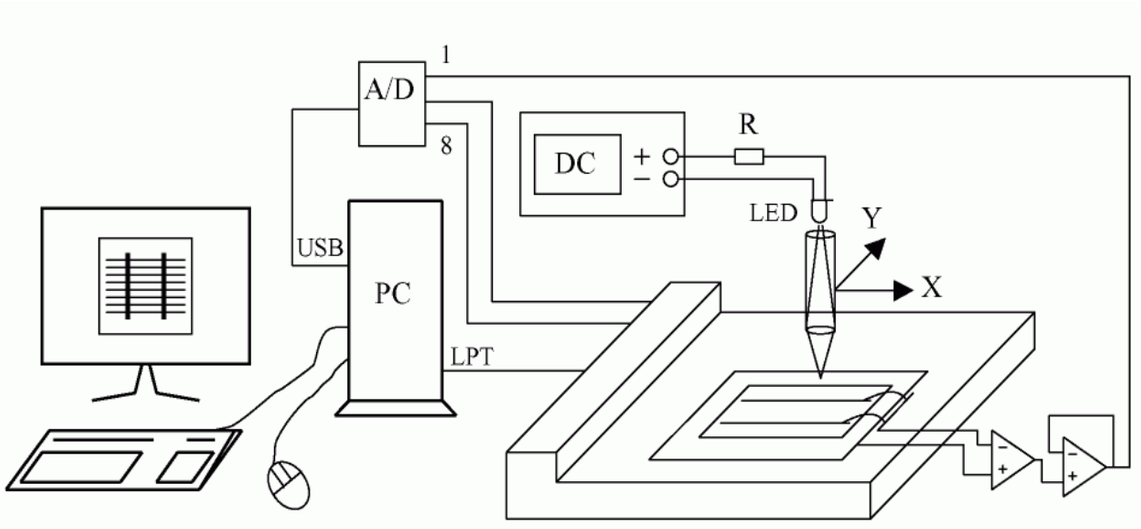

Fig. 1. Diagrammatical demonstration of measuring system (Vanek J, Fort T, 2007)

If the inner resistance of the measured amplifier is set to high value then the response of light is matching to V_{OC} and the method is designed as LBIV. There was some attempt to track the local maximum power point and to record local power value (LBIP) but the most widespread method is LIBC for this predicative feature. In such current map is possible to determine majority of local defects, therefor the LBIC is the useful method to provide a non-destructive characterization of structure of solar cells.

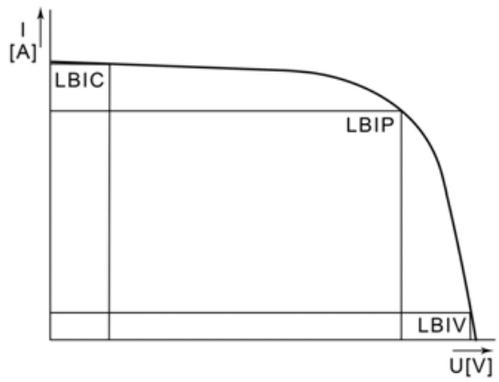

Fig. 2. Operating point of measuring amplifier and resultant method

1.1 Different wavelengths of light source used in LBIC

The effect on the absorption coefficient and penetration depth, defined as distance that light travels before the intensity falls to 36% (1/e), is clearly shown in figure 3. Note that the data in figure 3 represent unstrained bulk material with no voltage applied. By introducing strain or electrical bias, it is possible to shift the curves slightly to a higher wavelength due to a reduction in the effective band gap.

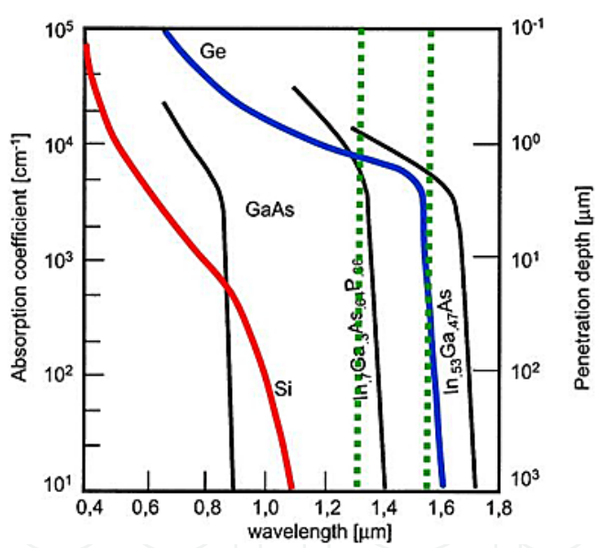

Fig. 3. Absorption coefficient and penetration depth of various bulk materials as a function of wavelength. (Intel,Photodetectors, 2004)

In cases where the photon energy is greater than the band gap energy, an electron has a high probability of being excited into the conduction band, thus becoming mobile. This interaction is also known as the photoelectric effect, and is dependent upon a critical wavelength above which photons have insufficient energy to excite or promote an electron positioned in the valence band and produce an electron-hole pair. When photons exceed the critical wavelength (usually beyond 1100 nanometres for silicon) band gap energy is greater than the intrinsic photon energy, and photons pass completely through the substrate. Table 1 lists the depths (in microns) at which 90 percent of incident photons are absorbed by a typical solar cell.

Wavelength (Nanometers)	400	450	500	550	600	650	700	750
Penetration Depth (Micrometers)	0.1	0.4	0.9	1.5	2.4	3.4	5.2	7.0
Wavelength (Nanometers)	750	800	850	900	950	1000	1050	1100
Penetration Depth (Micrometers	8.4	11	19	33	54	156	613	2857

Table 1. Photon Absorption Depth in Silicon (c-Si PC1D 300K)

On the other hand when the wavelength is closer to energy of band gab the spectral efficiency is higher. When photon with high energy impacts silicon atom there is high probability to excitation of valence electron to non-stable energy band and in short time the electron is moving to lower stable energy band. The energy difference is lost and change to heat. Therefor spectral response of higher wavelength photons should be higher than of photons of lower wavelength (even they have higher energy).

2. Light beam induced current measurement

Light sources with wavelengths of various colors were used for scanning of samples – Table 2. Various wavelengths of light were used to show the different defects in different depth under the surface of silicon solar cells. See Table 1. Apart from laser, highly illuminating LED diodes installed in a tube similar to that of LASER were used. The tube was a capsule enabling smooth installation of the LED diode instead of laser. It also enabled regulation of illumination.

The LBIC method is realized by the movement of the light source (focused LED diode or laser) fixed on the grid of the pen XY plotter MUTOH IP-210 near the solar cell surface. Thanks to the local response of the solar cell to incident light we get the scan of local current differences (we were using the measurement PC card Tedia PCA-1208). From the obtained data we can get the whole picture of the solar cell current response to light. From this picture we can read the most local type of defect.

For light exposure LASERs and high luminous LED diodes were used. They were inserted into a special container with the same dimensions like the LASERs. The container was used for smooth assembling in the same grid like the LASER and for holding the focusing lens and screening slide.

We have studied set of four samples of solar cells with known defects like swirl defect, scratches, diffusion fail and missing contacts act.

All global parameters of these test cells were known from previous measurements. These parameters are showed in Table 3.

source	laser	LED	LED	LED
color	infrared	red	green	blue
wavelength	830 nm	660 nm	560 nm	430 nm

Table 2. Used light sources

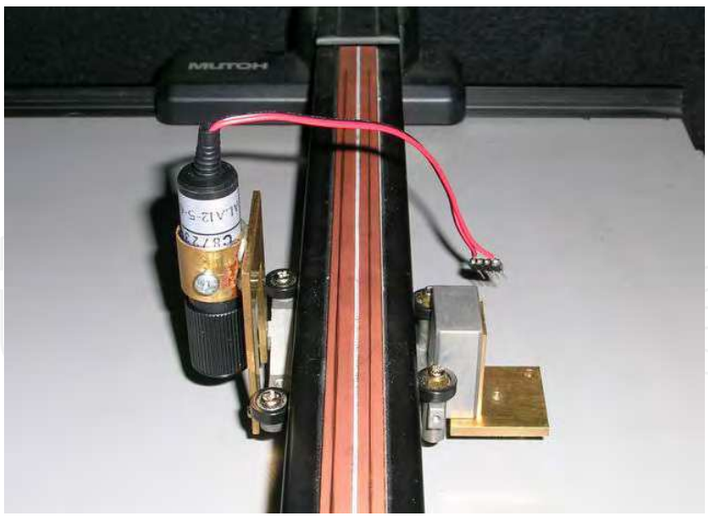

Fig. 4. Laser used in LBIC

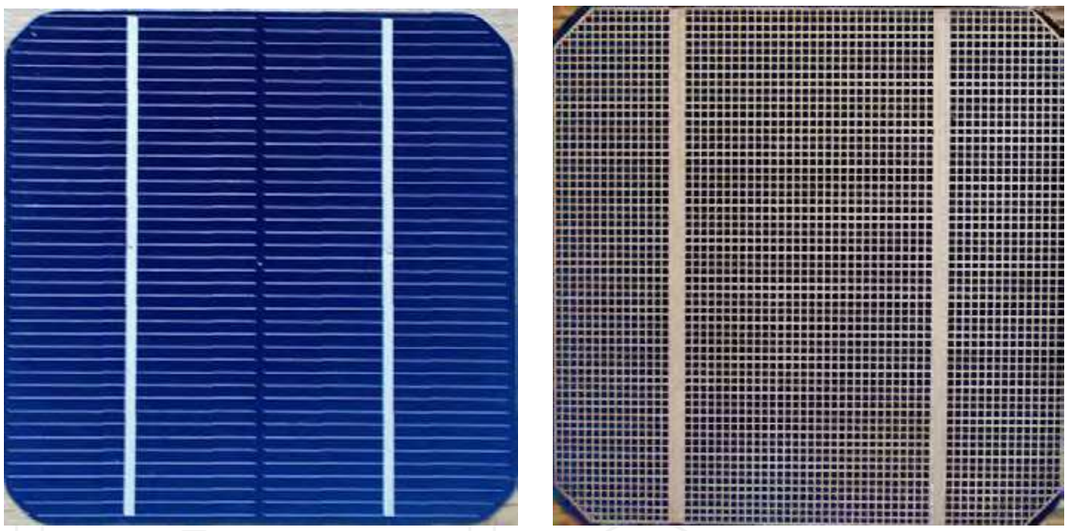

Fig. 5. Front and back side of monocrystaline silicon solar cell.

Sample	I_{450} [A]	I_{sc} [A]	U_{oc} [V]	I_m [A]	U_m [V]	P_m [W]	FF [%]	EEF [%]
1	2,729	2,842	0,576	2,628	0,476	1,252	76,5	12,04
2	2,344	2,511	0,559	2,293	0,461	1,057	75,4	10,17
3	2,426	2,602	0,560	2,344	0,466	1,092	74,9	10,50
4	2,500	2,670	0,567	2,473	0,459	1,136	75,1	10,92

Table 3. Data for global parameters of tested solar cells (Solartec s.r.o, 2005)

There are presented two results for each wavelength (colour of light) of inducing radiation to the chosen samples for a better comparison. There were the sample no. 1 and no 3 chosen. The maximal value of local current is assigned the white color and the minimal current

response is assigned black color. For authenticity of measurement the pictures are kept in their original setting.

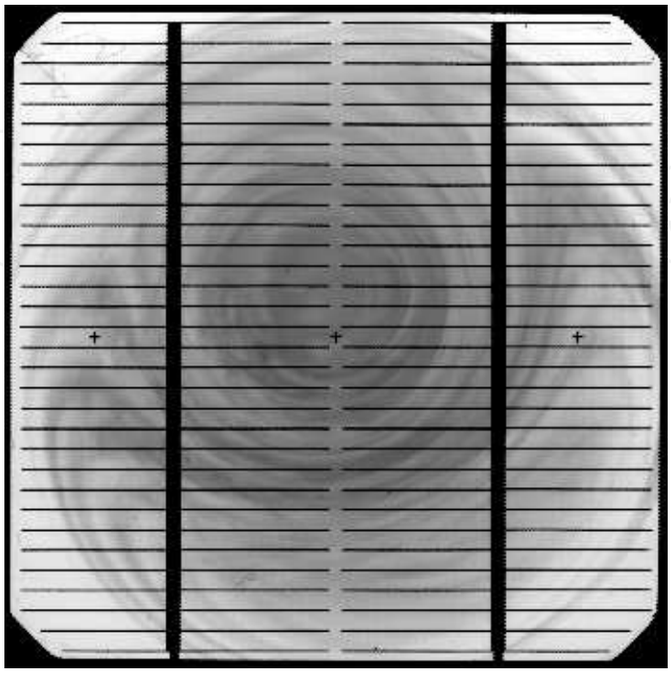

Fig. 6. Analyses of output local current of the sample no. 1 by usage of focused LED diode with middle wavelength 650 nm (red LED, T=297 K)

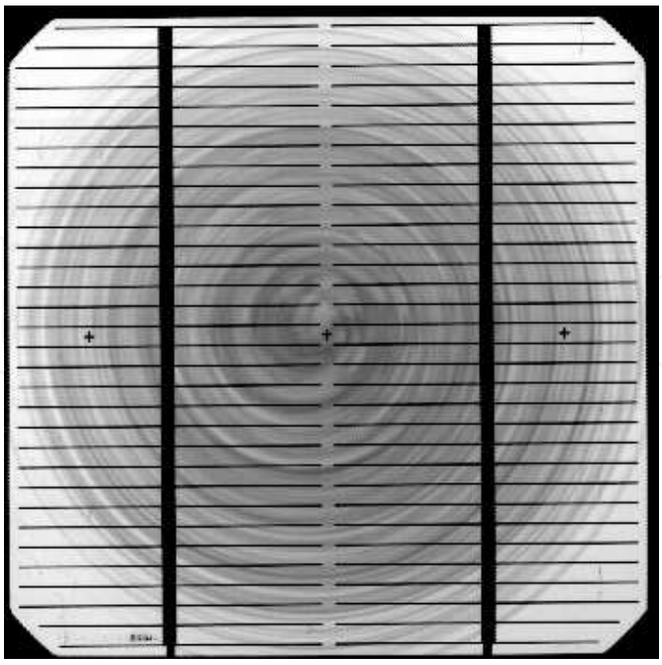

Fig. 7. Analyses of output local current of the sample no. 3 by usage of focused LED diode with middle wavelength 650 nm (red LED, T=297 K)

As mentioned above all samples contain a swirl defect. If you look at the pictures produced by red LED (wavelength 650 nm, figs 6 and 7) this defect is clearly visible.

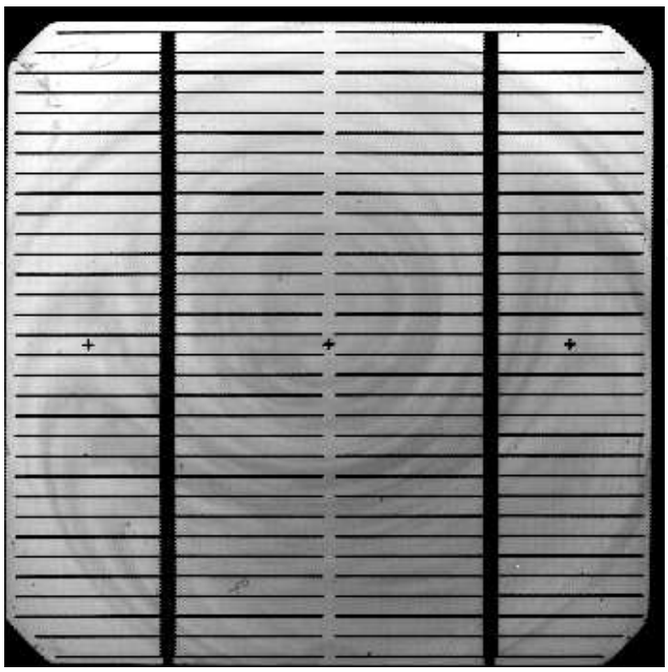

Fig. 8. Analyses of output local current of the sample no. 1 by usage of focused LED diode with middle wavelength 560 nm (green LED, T=297 K)

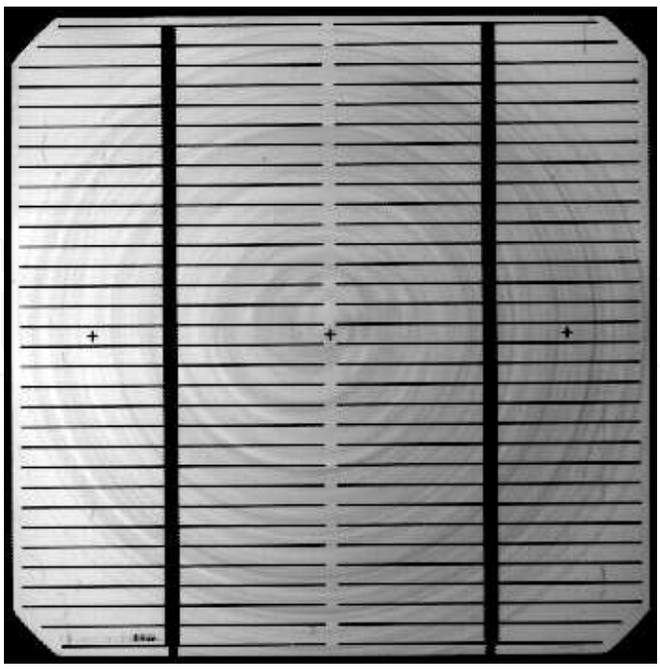

Fig. 9. Analyses of output local current of the sample no. 1 by usage of focused LED diode with middle wavelength 560 nm (green LED, T=297 K)

For the green LED diode (middle wavelength 560 nm, figures 8 and 9) the defect is still well visible, but not as well-marked as for the red colour (middle wavelength 650 nm).
From the principle of photovoltaic effect it is clear that the light with sufficiently long wavelength passes through the solar cell without generation of photocurrent. With a shorter wavelength the light is absorbed faster from impact light to solar cell and that is why the penetration depth is shorter.
The wavelength of red light is the longest for the used light sources; therefore the penetration depth is the longest. This is proven by well-market visibility of swirl defect which is the defect made in bulk of material.
Along the way the wavelength of blue light is the shortest and it causes the full loss of visibility of this defect. This is caused by the absorption of the light near the solar cell surface where the swirl defect is not taking effect yet.
The wavelength of green color light is between the wavelengths of red and blue color light. Therefore the green color light penetrates to a deeper depth than the blue color light but not so deep as the red color light.
The swirl defect for the blue color (wavelength 430 nm, figures. 10 and 11) is almost invisible.
We may think that the blue color light is not important for LBIC diagnostic because it does not allow the bulk defect detection. If you look at the figure closely, you can observe a decreased affectivity of solar cell in the top right-hand corner of solar cell no 3. (the area of dark gray). These inhomogeneities are due to irregular diffusion during solar cell manufacturing. By the usage of light of red color spectrum this defect is not possible to detect. These defects are surface defects. Even the green colour light can make these inhomogeneities visible, but they can be easily overlooked.

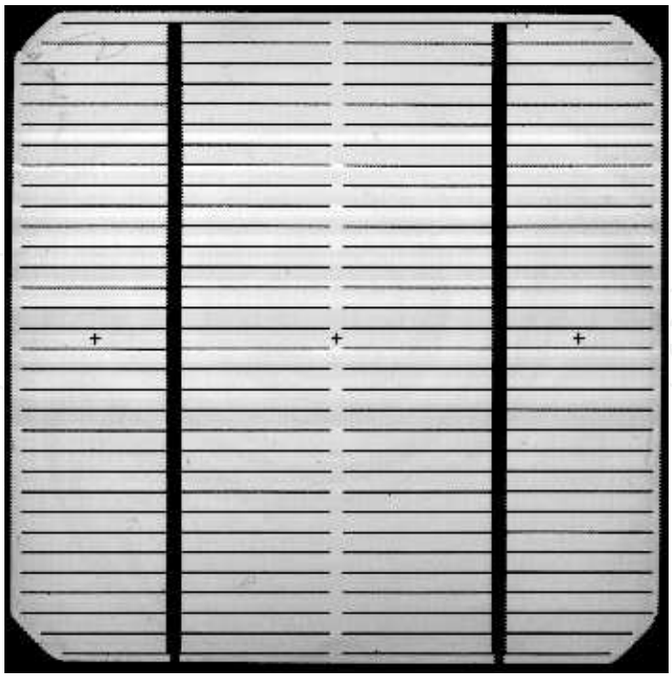

Fig. 10. Analyses of output local current of the sample no. 1 by usage of focused LED diode with middle wavelength 430 nm (blue LED, T=297 K)

Fig. 11. Analyses of output local current of the sample no. 3 by usage of focused LED diode with middle wavelength 430 nm (blue LED, T=297 K)

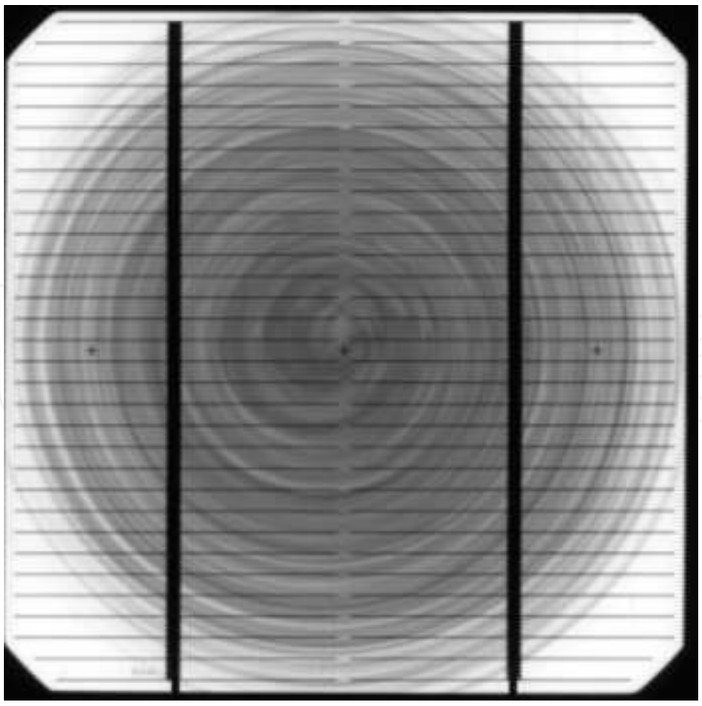

Fig. 12. Analyses of output local current of the sample no. 3 by usage of focused infrared laser (830nm, T=297K)

Among other defects we count scratches and scrapes which are well-marked by all colors even if they are surface defects. This is due to the damage of solar cell structure by higher recombination or higher reflection of damaged surface.
We can compare results for sample no. 3 with the figure produced by the infrared laser M4LA5-30-830 (wavelength 830nm, Fig. 12.). This is the longest wavelength and the penetration depth is the deepest.
The swirl defect displayed by the infrared laser is the most intensive which is the proof of the deepest penetration depth. The obtained picture is slightly defocused in comparison with previous pictures. This is due complicated focusing system of impacting beam because IR light is not visible. The focusing is performed by a special specimen used for focusing the IR laser. The big intensity of defect and a little defocused picture produce a partial loss of information about the surface defect.

2.1 Graphic analyses of LBIC data

The result of solar cell scanning is array of values corresponding to local current response to impacting light beam. This array of value is depending on AD convertor but mostly the result is the 12-bit value matrix which is converted to 8 bit (grey tone picture) graphic output. A value 0 corresponds to the darkest black and value 255 corresponds to the lightest white. By the changing of the corresponding colour interval we can visualize the defects which are hidden for graphic analyse and improve the output picture.

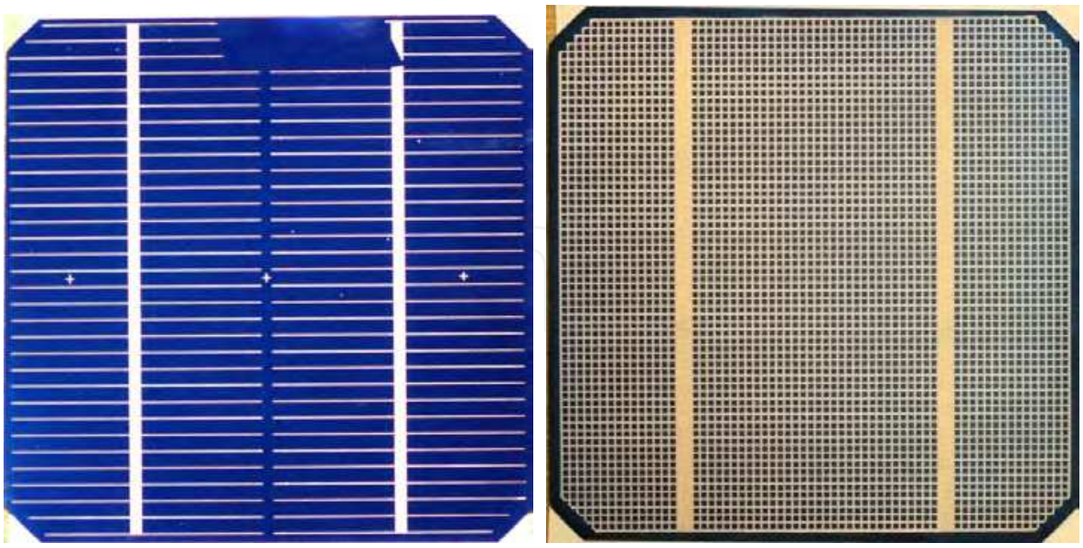

Fig. 13. Front and back side of tested monocrystaline silicon solar cell 710B1.

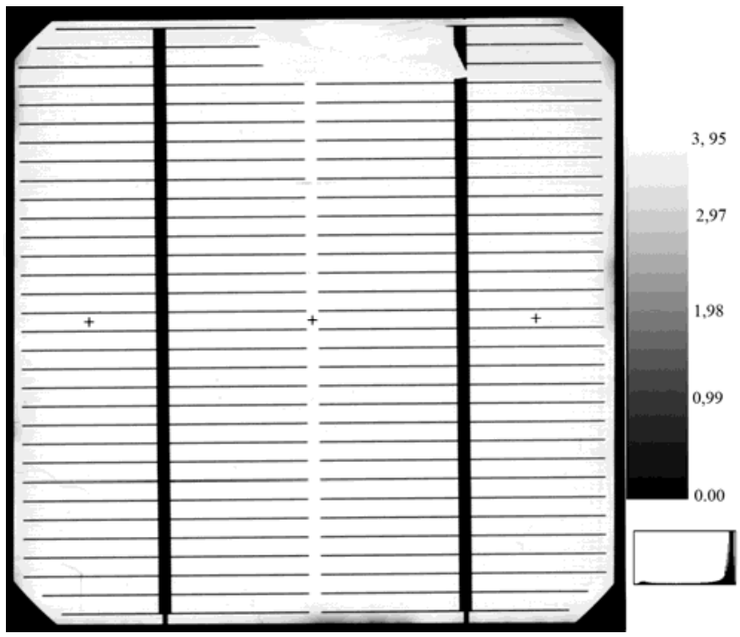

Fig. 14. Output LBIC scan of sample 710B1 in maximal converted interval measured values to grey tone colour (T = 298 K, λ_S = 650 nm)

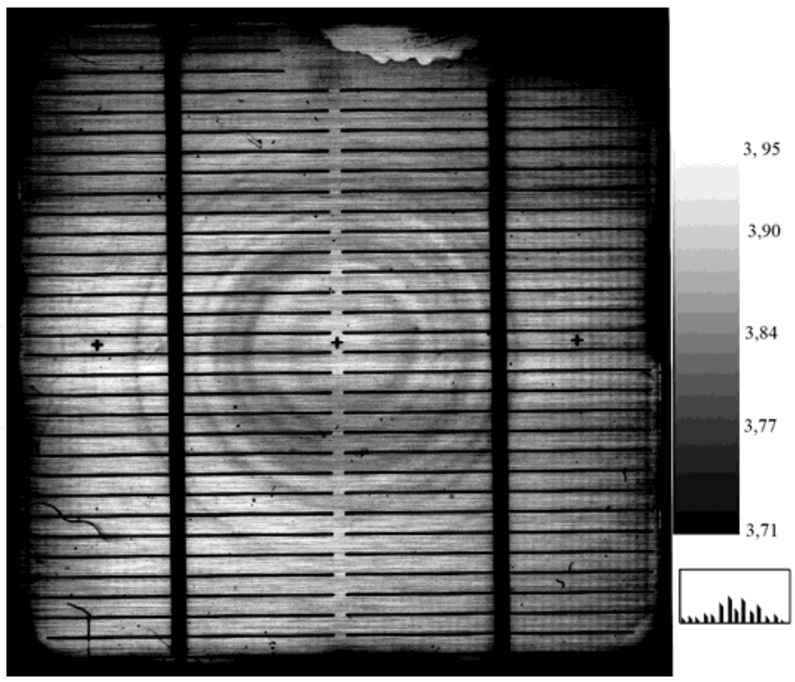

Fig. 15. Output LBIC scan of sample 710B1 in linear selected interval measured values of 3.71 to 3.91 grey tone colour (T = 298 K, λ_S = 650 nm)

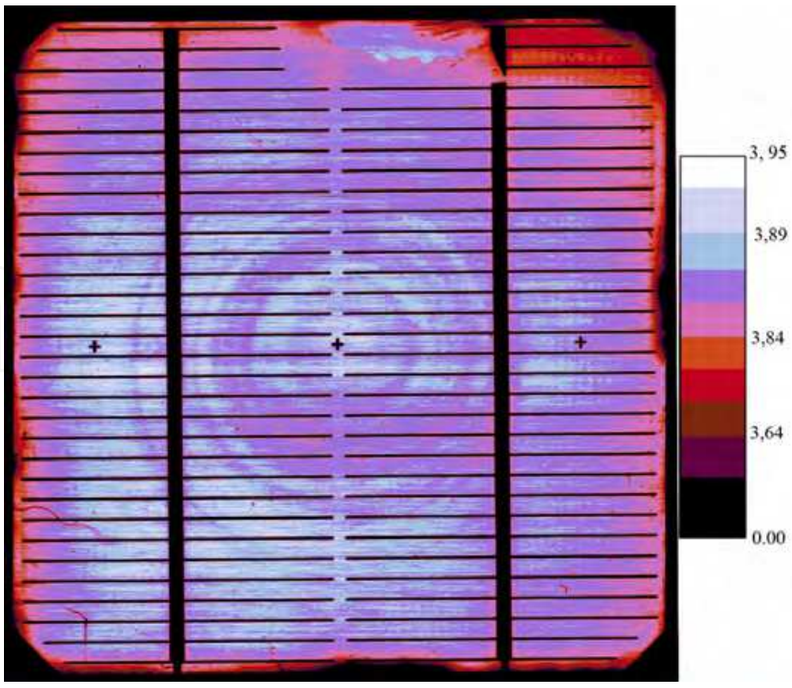

Fig. 16. Output LBIC scan of sample 710B1 in coloured nonlinear selected interval measured values of 0 to 3.95 grey tone colour (T = 298 K, λ_S = 650 nm)

3. Projection of solar cell back side contact to the LBIC image

Thanks to different wavelength of used light illumination we can detect different defect and structures depending on penetration depth of light photon. However, the experiments have showed that we can detect structures behind of expected depth like contact bar on the back side of solar cells. This contact we did not detect using long wavelength (IR-980 nm or red-630 nm LED) but they were clearly visible using short wave length (green-525 nm, blue-430 nm or UV-400 nm LED). Nevertheless using long wavelength enable to clearly detect deep material defects like swirl which are not clearly detectable by UV or blue wavelength but this wavelength enables to detect surface defect.

Projection of back side contact bar to short wavelength LBIC picture can be explain by theory of secondary emission of long wavelength light (~1100 nm) which has penetration depth (~2800μm) much more higher then solar cells depth. Incident high energy light is absorbed in front surface of solar cell and generates electron-hole pair. Part of this carrier charges are separated and generated photocurrent. Because of small penetration depth of impacting photon, most of carrier charges generate near surface area. Thank to high recombination rate on surface a big amount of this carrier charges recombine and emit IR light. The spectral efficiency of impacting photon wavelength is low so the output primary photocurrent is low, too, and do not cover the current induced by secondary emitted photons with energy near silicon band gap and with high spectral efficiency. IR light incidents on back metal contact are absorbed without generation electron-hole pair. Light incident to back surface without metallic contact is reflected back and is absorbed inside substrate volume. This theory was verify by scanning of solar cell illuminated by UV light (Fig. 18) in IR region (Fig. 19).

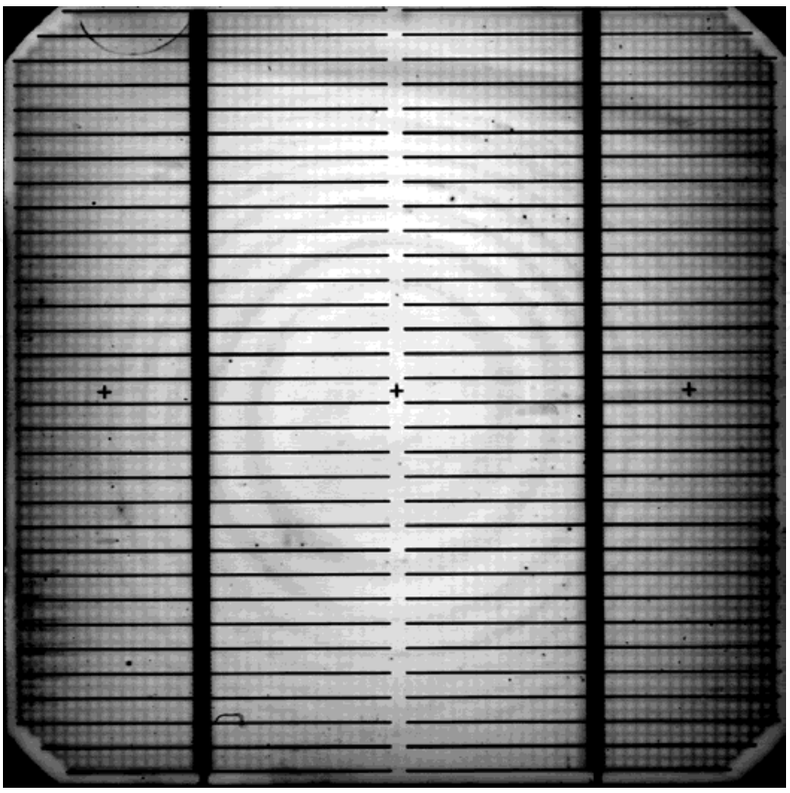

Fig. 17. Projection of back contact bar in LBIC of the sample 57A3 by usage of focused LED diode with middle wavelength 430 nm (blue LED, T=297 K)

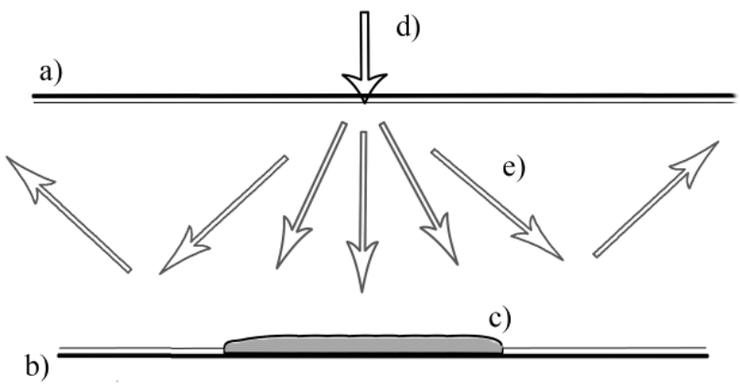

Fig. 18. Theory of projection back side contact during secondary emission of long wavelength light.
a) front side surface, b) back side surface, c) metallic contact on back side, d) short wavelength light e) emitted long wavelength light.

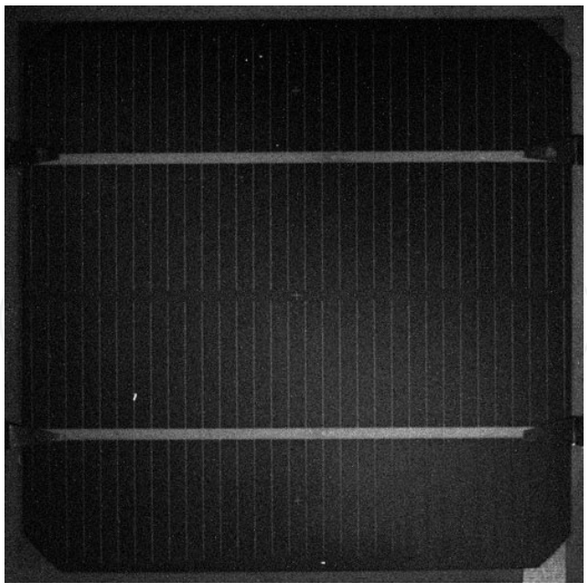

Fig. 19. Photoluminescence of solar cell 24B3 illuminated by UV-400 nm light, scan through blue filter (380- 460nm) – no strong luminescence.

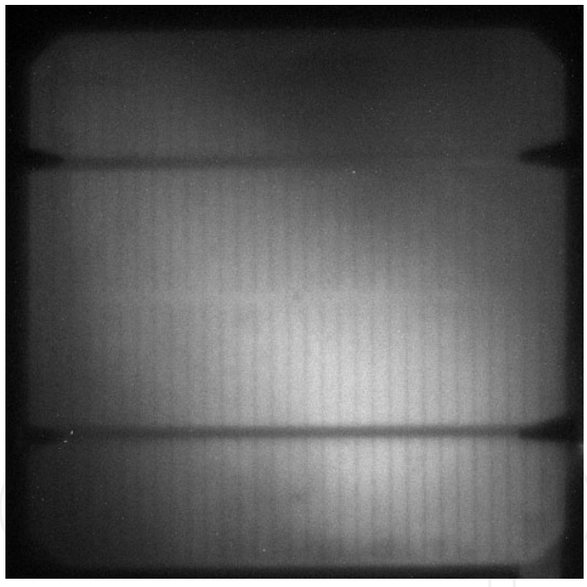

Fig. 20. Photoluminescence of solar cell 24B3 illuminated by UV-400 nm light, scanned through IR filter (742 nm and more) - measurable luminescence.

4. Conclusion

The measurement of solar cells using the LBIC method makes possible to most type of defect detection. Various wavelengths of light were used to spot different defects at different depths under the surface of silicon solar cells. This chapter presents the LBIC analysis of set silicon solar cells prepared up-to-date technique. The measurements have demonstrated a strong dependence of LBIC characteristics on the used light source wavelength.

Even better results could be achieved by using LASERs instead of focused LED diodes. The problem of using LED diodes is the weak intensity of light beam connected with low photocurrent and superposition with surrounding noise.

5. Acknowledgement

This research and work has been supported by the project of CZ.1.05/2.1.00/01.0014 and by the project FEKT-S-11-7.

6. References

Vasicek, T. Diploma theses, 2004, Brno University of Technology, Brno

Pek, I. Diploma theses , 2005, Brno University of Technology, Brno

Intel, Photodetectors, On-line : http://www.intel.com/technology/itj/2004/ volume08issue02/ art06_siliconphoto/p05_photodetectors.htm, Citeted 2004

Vanek, J., Brzokoupil, V., Vasicek, T., Kazelle, J., Chobola, Z., Barinka, R. The Comparison between Noise Spectroscopy and LBIC In *The 11th Electronic Devices and Systems Conference. The 11th Electronic Devices and Systems Conference*. Brno: MSD, 2004, s. 454 - 457, ISBN 80-214-2701-9

Vaněk, J., Kazelle, J., Brzokoupil, V., Vašíček, T., Chobola, Z., Bařinka, R. The Comparison of LBIC Method with Noise Spectroscopy. Photovoltaic Devices. Kranjska Gora, Slovenia, *PV-NET*. 2004. p. 60 - 60.

Vaněk, J.; Chobola, Z.; Vašíček, T.; Kazelle, J. The LBIC method appended to noise spectroscopy II. In *Twentieth Eur. Photovoltaic SolarEnergy Conf*. Barcelona, Spain, WIP-Renewable Energies. 2005. p. 1287 - 1290. ISBN 3-936338-19-1.

Vaněk, J., Kazelle, J., Bařinka, R. Lbic method with different wavelength of light source. In *IMAPS CS International Conference* 2005. Brno, MSD s.r.o. 2005. p. 232 - 236. ISBN 80-214-2990-9.

Vaněk, J., Kubíčková, K., Bařinka, R. Properties of solar cells by low an very low illumanation intensity. In *IMAPS CS International Conference* 2005. Brno, MSD s.r.o. 2005. p. 237 - 241. ISBN 80-214-2990-9.

Vaněk, J., Boušek, J., Kazelle, J., Bařinka, R. Different Wavelenghts of light source used in LBIC. In *21st European Photovoltaic Solar Energy Conference*. Dresden, Germeny, WIP-Renewable Energies. 2006. p. 324 - 327. ISBN 3-936338-20-5.

Vaněk, J.; Fořt, T.; Jandová, K. Solar cell back side contact projection to the front side lbic image. In *8th ABA Advanced Batteries and Accumulators*. Brno, TIMEART agency. 2007. p. 253 - 255. ISBN 978-80-214-3424-0.

Vaněk, J.; Fořt, T.; Jandová, K.; Bařinka, R. Projection fo solar cell back side contact to the LBIC image. In *EDS'07*. Brno, TIMEART agency. 2007. p. 253 - 255. ISBN 978-80-214-3470-7.

Vaněk, J.; Dolenský, J.; Jandová, K.; Kazelle, J. Dynamic light beam induced voltage testing method of solar cell. In *EDS ´08 IMAPS Cs International Conference Proceedings*. Brno, Vysoké učení technické v Brně. 2008. p. 153 - 156. ISBN 978-80-214-3717-3.

Vaněk, J.; Jandová, K.; Kazelle, J.; Bařinka, R.; Poruba, A. Secondary photocurrent, current generated from secondary emitted photons. In *23rd European Photovoltaic Solar Energy Conference*, 1-5 September 2008, Valencia, Spain. 2008. p. 323 - 325. ISBN 3-936338-24-8.

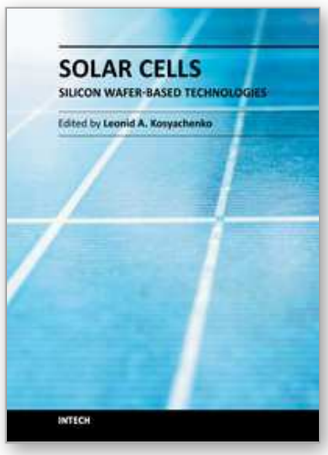

Solar Cells - Silicon Wafer-Based Technologies

Edited by Prof. Leonid A. Kosyachenko

ISBN 978-953-307-747-5
Hard cover, 364 pages
Publisher InTech
Published online 02, November, 2011
Published in print edition November, 2011

The third book of four-volume edition of 'Solar Cells' is devoted to solar cells based on silicon wafers, i.e., the main material used in today's photovoltaics. The volume includes the chapters that present new results of research aimed to improve efficiency, to reduce consumption of materials and to lower cost of wafer-based silicon solar cells as well as new methods of research and testing of the devices. Light trapping design in c-Si and mc-Si solar cells, solar-energy conversion as a function of the geometric-concentration factor, design criteria for spacecraft solar arrays are considered in several chapters. A system for the micrometric characterization of solar cells, for identifying the electrical parameters of PV solar generators, a new model for extracting the physical parameters of solar cells, LBIC method for characterization of solar cells, non-idealities in the I-V characteristic of the PV generators are discussed in other chapters of the volume.

INTECH
open science | open minds

InTech Europe
University Campus STeP Ri
Slavka Krautzeka 83/A
51000 Rijeka, Croatia
Phone: +385 (51) 770 447
Fax: +385 (51) 686 166
www.intechopen.com

InTech China
Unit 405, Office Block, Hotel Equatorial Shanghai
No.65, Yan An Road (West), Shanghai, 200040, China
中国上海市延安西路65号上海国际贵都大饭店办公楼405单元
Phone: +86-21-62489820
Fax: +86-21-62489821

IntechOpen